Dynamic Light Scattering Study of Gelatin−Surfactant Interactions

A. Saxena, T. Antony, and H. B. Bohidar*

School of Physical Sciences, Jawaharlal Nehru University, New Delhi-110 067, India

Received: August 5, 1997; In Final Form: February 25, 1998

Binding of anionic (sodium dodecyl sulfate, SDS), cationic (cetyl trimethyl ammonium bromide, CTAB), and nonionic (TX-100) surfactants to gelatin chains in aqueous buffer (pH = 7.0) medium has been studied by dynamic light-scattering technique performed at $T = 30$ °C. In the surfactant concentration range varying from 0 to 100 mM, SDS exhibited electrostatic binding to the charged groups of the polypeptide chain resulting in considerable reduction in the hydrodynamic radius (R_h) of gelatin up to the critical association concentration (CAC), and at higher concentrations both the SDS micelles and gelatin−SDS complexes were found to be coexisting in equilibrium. In the case of CTAB, almost the opposite was observed: the gelatin chains showed small increase in size up to the CAC. Beyond this, the gelatin−CTAB complexes were observed to grow significantly, and these were found to be in equilibrium with CTAB micelles. TX-100 exhibited little hydrophobic binding to gelatin, and no observable change in gelatin size was observed. The micellar shapes were found to be near-spherical for SDS and oblate ellipsoidal for CTAB micelles. Results have been explained through the necklace-bead model of polymer−surfactant interactions.

I. Introduction

The study of surfactant−polymer interaction is of great interest for many physicochemical as well as biological phenomena. Polymer−surfactant systems which have been investigated by a variety of experimental techniques were reviewed by Robb[1], Goddard,[2] and recently by Kwak and Hayakawa.[3] These interactions bring significant changes in the conformation and properties of the polymer. Nagarajan[4] discussed six possible types of associations involving either individual surfactant molecules or surfactant micelles. NMR[5] and neutron-scattering[6] studies suggest the existence of polymer−micelle complexes. When both the polymer and surfactant are charged, the interactions are mostly coulombic in nature. The most widely used surfactant is SDS, and considerable effort has been made in the past to study its interaction with a variety of polymers and biopolymers.[7−11] Relatively few studies have been done with cationic and non-ionic surfactants.[12] SDS is known to induce denaturations in many proteins.[13−15] These studies reveal that ligands like surfactants bind to proteins in four successive steps. At low surfactant concentrations, specific binding occurs predominantly at high-energy binding sites on the protein. This is followed by a non-cooperative region where binding of ligand to protein is rather marginal. At higher concentrations of the surfactant there is a propensity for cooperative binding leading to (in most cases) protein unfolding. Beyond this region, addition of excess surfactant does not effect the over all size of the protein−ligand complex and mostly micellar formation dominates the picture. This defines the saturation binding for low molecular weight proteins like BSA, under saturation binding conditions typically 1 g of protein binds to ∼1.5 g of surfactant. For longer polypeptides, this binding ratio can be significantly different.

Here we have investigated the interaction between a high molecular weight polypeptide (gelatin) and various surfactants (i) sodium dodecyl sulfate (SDS), (ii) cetyl trimethyl ammonium bromide (CTAB), and (iii) Triton X-100 (TX-100). Gelatin which is denatured collagen is a cheap and readily available polypeptide. Some of the earlier studies on gelatin-surfactant are those by Pankhurst,[16] Knox and Wright,[17] Kragh,[18] and Shone.[19] Kragh and Knox used surface-tension technique to study interactions above the IEP (iso electric point), whereas Knox and Wright studied precipitation phenomena in a gelatin−SDS system below the IEP using the turbidity method. Greener et. al.[20] studied the binding of gelatin to a variety of surfactants ranging from ionic to nonionic nature using viscometric methods and concluded that the extent of interaction was closely related to surfactant type, surfactant−gelatin composition, and ionic strength of the solution, with lesser effects exerted by gelatin type and pH level.

The method used in our work is dynamic light-scattering technique (**DLS**), which is a powerful tool for the investigation of the structure and dynamics of polyelectrolyte solutions. To the best of our knowledge gelatin interaction with cationic and nonionic surfactant using DLS has not been reported anywhere.

II. Experimental Procedures

(i) Materials. Gelatin was purchased from M/s Loba-Chemie (Indo-Astranal Co., India). Double distilled water was used for dissolving the gelatin powder. The pH was adjusted to 7.0 using a sodium citrate/sodium chloride buffer. Gelatin solutions were prepared by soaking the gelatin powder in buffer for ∼1 h followed by heating up to 50 °C with mild stirring. Gelatin concentration used for the present study was 0.5% (w/v). SDS was procured from SISCO Research Laboratories, (India), CTAB, and TX-100 from M/s Loba-Chemie (India) were used. Solutions (1 M)of all the three surfactants were prepared in double distilled water.

(ii) Methods. The light scattering apparatus consisted of a laboratory goniometer with two arms. The excitation source was a He−Ne laser (Aerotech, 10 mW) mounted on the fixed arm of this goniometer and a photomultiplier tube (Thorn EMI Model B2FBK/RFI) was mounted on the other arm. The DLS

* Corresponding author. Fax: +91-11-616 5886 and +91-11-619 8324. E-mail: bohidar@jnuniv.ernet.in.

S1089-5647(97)02556-X CCC: $15.00
Published on Web 06/05/1998

experiments were carried out at scattering angle fixed at 90°. Gelatin sample (2 mL) was taken in a 5 mL cylindrical quartz cell and was held inside a homemade temperature controller.[21] This controller provided temperature regulation in the range of 15−75 °C with an accuracy of ±0.1 °C. Scattered light from the sample was detected by the photomultiplier tube, and the photocurrent was suitably amplified and digitized before it was fed to a 1024 channel digital photon correlator (Brookhaven BI-9000 AT, U.S.A.). The whole scattering appratus was installed on a vibration isolation table.

To vary the concentration of surfactant in gelatin solution, calculated volumes of 1 M surfactant corresponding to 2 mL of gelatin were added directly to the gelatin sample kept in the quartz cell using a microlitre syringe and the mixture was mildly stirred. The concentration range was varied from below the CMC to above the CMC. All the experiments were done at 30 °C. Our gelatin sample has been found to be a sol at this temperature.[22,23] Correlograms were recorded when the desired temperature was reached. Time duration for recording each correlogram was 30 min, and over this duration, the temperature was observed to have remained steady within the accuracy of experimental error.

(ii) DLS Data Analysis. For scatterers undergoing Brownian dynamics in a solvent environment, the field autocorrelation function $g_1(\tau)$ is given as

$$g_1(\tau) = g_1(0)e^{-D_T q^2 \tau} \quad (1)$$

where D_T is the average translational diffusion coefficient of the particles and the scattering wave vector $q = 4\pi n\lambda^{-1} \sin \theta/2$, where n is the refractive index of the solution, θ the scattering angle, and $\lambda = 6328$ Å is the wavelength of the excitation source. In fact, $(2\pi/q)$ defines the length scale over which the sample is being probed. The prefactor $g_1(0) \leq 1$ defines the signal-to-noise ratio in the scattering experiment, and it is also called the coherence area factor. The expression for $g_1(\tau)$ remains valid for monodisperse samples or for samples with low polydispersity, but only for situations where the molecular weight distribution is unimodal. Equation 1 can be expanded in a Taylor series following Koppel's formulation, and the average diffusity D_z and polydispersity can be deduced from this analysis.[24]

If there are N_i moles of species i with molecular weight M_i, and diffusion coefficient D_i, D_z is defined as

$$D_z = \frac{\sum_i D_i N_i M_i^2}{\sum_i N_i M_i^2} \quad (2)$$

Consequently, polydispersity P is defined as

$$P = \frac{\langle (D_z - \bar{D}_z)^2 \rangle}{(\bar{D}_z)^2} \quad (3)$$

Further details of this discussion can be found elsewhere.[24] In case of bimodal distributions $g_1(\tau)$ can be wirtten as

$$g_1(\tau) = g_{11}(0)e^{-D_{1T} q^2 \tau} + g_{12}(0)e^{-D_{2T} q^2 \tau} \quad (4)$$

where $g_{11}(0)$ and $g_{12}(0)$ have identical meaning as $g_1(0)$; D_{1T} and D_{2T} are translational diffusion coefficients of first and second types of scattering particles and both of these are individually polydisperse.

TABLE 1: Gelatin + SDS[a]

SDS conc (mM)	$D_{com} \times 10^{-8}$ (cm^2 s)	R_c (Å)	$D_{mic} \times 10^{-8}$ (cm^2 s^{-1})	R_M (Å)	polydispersity P
0.0	2.02 ± 0.08	200 ± 10			0.22
0.5	2.39 ± 0.08	169 ± 10			0.21
1.0	2.30 ± 0.08	175 ± 10			0.28
2.0	2.47 ± 0.08	163 ± 10			0.27
4.0	2.88 ± 0.08	140 ± 10			0.19
8.0	3.03 ± 0.09	133 ± 8	14.3 ± 0.6	29 ± 2	0.32
15.0	2.24 ± 0.09	180 ± 10	25.0 ± 0.6	16 ± 1	0.30
20.0	2.07 ± 0.08	195 ± 10	26.5 ± 0.8	15 ± 1	0.36
40.0	1.74 ± 0.09	229 ± 15	33.9 ± 0.9	12 ± 1	0.33
80.0	1.45 ± 0.08	278 ± 15	29.2 ± 0.8	14 ± 1	0.33
100.0	1.41 ± 0.07	286 ± 15	22.2 ± 0.8	18 ± 2	0.25

[a] Values of the translational diffusion coefficient of gelatin + SDS complexes (D_{com}), formed in aqueous solutions and the corresponding hydrodynamic radii values (R_c) at $T = 30$ °C. Above CMC, micelles were formed; the diffusivities of micelles (D_{mic}) and their corresponding hydrodynamic radii (R_m) values are listed. The polydispersity as obtained from CONTIN analysis are shown in the last column.

TABLE 2: Gelatin + CTAB[a]

CTAB conc (mM)	$D_{com} \times 10^{-8}$ (cm^2 s^{-1})	R_c (Å)	$D_{mic} \times 10^{-8}$ (cm^2 s^{-1})	R_m (Å)	polydispersity P
0.0	1.95 ± 0.08	200 ± 10			0.33
0.05	1.96 ± 0.08	205 ± 10			0.32
0.1	2.02 ± 0.08	210 ± 10			0.31
0.2	1.97 ± 0.09	215 ± 10			0.31
0.4	2.08 ± 0.08	220 ± 10	16.8 ± 0.8	24 ± 2	0.20
0.8	1.77 ± 0.07	230 ± 12	15.3 ± 0.7	27 ± 2	0.32
1.0	1.64 ± 0.06	250 ± 12	15.6 ± 0.7	26 ± 2	0.31
4.0	1.49 ± 0.06	260 ± 15	13.8 ± 0.8	29 ± 2	0.22
8.0	1.35 ± 0.06	270 ± 10	16.68 ± 0.9	25 ± 2	0.34
20.0	1.30 ± 0.06	280 ± 15	14.16 ± 0.7	28 ± 2	0.18
40.0	1.22 ± 0.06	320 ± 15	13.11 ± 0.7	30 ± 2	0.38
80.0	1.12 ± 0.06	360 ± 20	10.51 ± 0.8	40 ± 3	0.18

[a] Values of the translational diffusion coefficient of gelatin + CTAB complexes (D_{com}), formed in aqueous solutions, and the corresponding hydrodynamic radii values (R_c) at $T = 30$ °C. Above CMC, micelles were formed; the diffusivities of micelles (D_{mic}) and their corresponding hydrodynamic radii (R_m) values are listed. The polydispersity as obtained from CONTIN analysis are shown in the last column.

The digital correlator measures the intensity autocorrelation function $g_2(\tau)$ related to the function $g_1(\tau)$ valid for a Gaussian scattering process through Siegert relation[24]

$$g_2(\tau) = A + B|g_1(\tau)|^2 \quad (5)$$

where A defines the background of the signal and B defines the signal modulation. In our experiments $g_2(\tau)$ were measured and reduced to $g_1(\tau)$ by subtracting the background. There were three experimental situations involving gelatin and surfactants (i) below CMC, (ii) at CMC, and (iii) above CMC. Here CMC refers to CMC of pure surfactant in aqueous medium. The data fitting was done using the following conjugation model:

(i) Below and at CMC: Gelatin + Surfactant $\rightleftharpoons$ $(\text{gelatin}-\text{surfactant})_{complex}$

(ii) Above CMC: Geltain + Surfactant $\rightleftharpoons$ $(\text{gelatin}-\text{surfactant})_{complex}$ + Micelles

Below and at CAC, the micelles of surfactant were unlikely to form, hence the correlation function $g_1(\tau)$ was fitted to a single exponential given by eq 1 using CONTIN regression software provided by Brookhaven Instruments (BIC, U.S.A.) which provided excellent fitting. The measured values of D_T for surfactant bound gelatin complexes are listed in Tables 1−3 along with their correponding polydispersity and hydrodynamic

TABLE 3: Gelatin + TX-100[a]

TX-100 conc (mM)	$D_{com} \times 10^{-8}$ ($cm^2\ s^{-1}$)	R_c (Å)	$D_{mic} \times 10^{-8}$ ($cm\ s^{-1}$)	R_m (Å)	polydispersity P
0.0	1.95 ± 0.08	220 ± 15			0.33
0.05	1.87 ± 0.08	225 ± 15			0.21
0.1	1.90 ± 0.08	215 ± 15			0.25
0.2	1.83 ± 0.07	220 ± 15			0.39
0.4	2.00 ± 0.07	215 ± 15	16.9 ± 0.8	15 ± 1	0.37
0.8	2.10 ± 0.07	195 ± 10	30.9 ± 0.9	14 ± 1	0.38
5.0	2.10 ± 0.08	205 ± 10	29.7 ± 0.9	14 ± 1	0.23
10.0	2.10 ± 0.08	215 ± 10	29.1 ± 0.9	14 ± 1	0.22
50.0	1.97 ± 0.08	220 ± 15	27.7 ± 0.9	15 ± 1	0.38

[a] Values of the translational diffusion coefficient of gelatin + TX-100 complexes (D_{com}), formed in aqueous solutions and the corresponding hydrodynamic radii values (R_c) at $T = 30$ °C. Above CMC, micelles were formed; the diffusivities of micelles (D_{mic}) and their corresponding hydrodynamic radii (R_m) values are listed. The polydispersity as obtained from CONTIN analysis are shown in the last column.

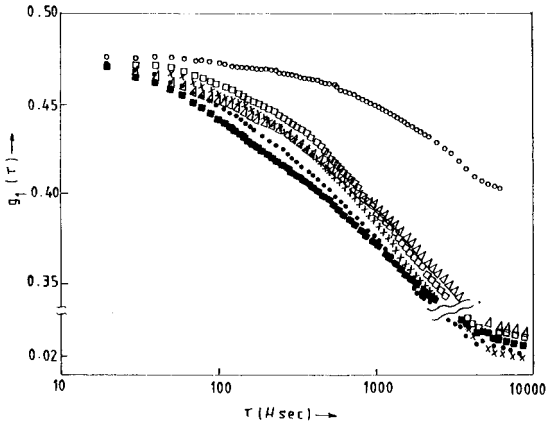

Figure 1. Normalized autocorrelation function $g_1(\tau)$ of gelatin + SDS solution as function of varying surfactant concentration at $T = 30$ °C. Open circles, squares, crosses, triangles, filled circles, and filled squares correspond to SDS concentrations of 0, 8, 20, 40, and 100 mM, respectively. Notice the sudden reduction in the relxation time of the correlation function when the SDS concentration was raised to 8 mM, implying shrinking of the gelatin chain. The double-exponential fitting accuracy was better than ±0.5% in all these cases.

radii values, R_h, deduced through the use of Stokes−Einstein relation

$$\bar{D}_z = \frac{k_B T}{6\pi\eta R_h} \tag{6}$$

where k_B is Boltzmann's constant and η is solvent viscosity at absolute temperature T. The data fitting to a single exponential function with the built-in effects of polydispersity was excellent in this domain.

For surfactant concentrations above CMC the single-exponential fitting was not found to be adequate and we resorted to double-exponential fitting using eq 4 with the software provided by BIC. Now we shall identify the D_{1T} as the diffusion coefficient of the gelatin−surfactant complex ($\bar{D}_{com}$) and D_{2T} as that of pure surfactant micelles ($\bar{D}_{mic}$).

III. Results and Discussions

A typical set of correlation functions are shown in Figure 1 for concentrations below and above CMC for the surfactant SDS. The measured parameters are listed in Tables 2−3 for all the three surfactants. The translational diffusion coefficients $\bar{D}_c$ of the complexes are plotted as a function of surfactant to gelatin concentration ratio in Figure 2 (below CMC) and Figure 3 (above CMC). The corresponding hydrodynamic radii values are plotted in Figures 4 and 5.

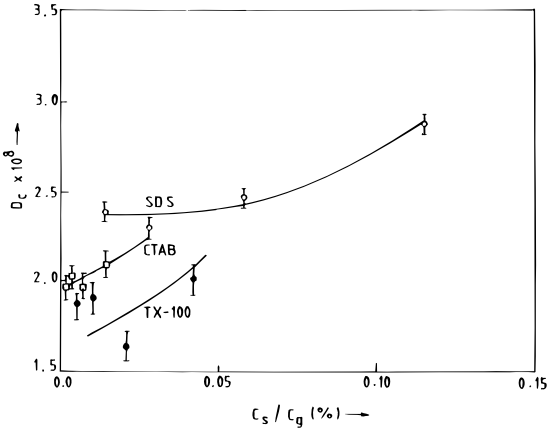

Figure 2. Translational diffusion coefficient (D_{com}) of gelatin−surfactant complexes at various relative concentration of surfactant. Gelatin concentration was 0.5% (w/v) at 30 °C. The solid lines are best fit to the data. For the TX-100 sample, the fitting is somewhat poor. Surfactant concentrations are less than the CMC values.

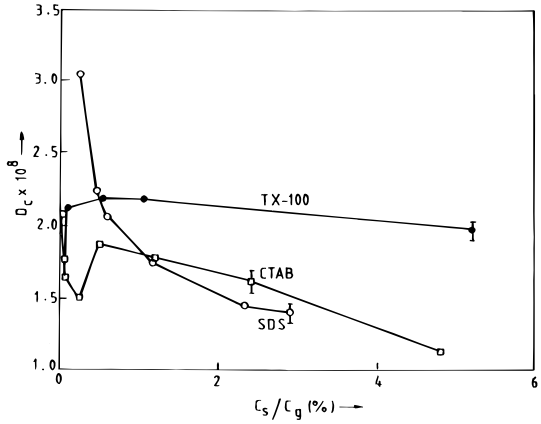

Figure 3. Translational diffusion coefficient (D_{com}) of gelatin−surfactant complexes at various relative concentration of surfactant. Gelatin concentration was 0.5% (w/v) at 30 °C. The solid lines are best fit to the data. Complete range of surfactant concentrations are shown here.

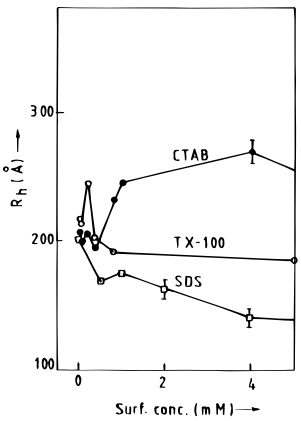

Figure 4. Hydrodynamic radius (R_h) of gelatin−surfactant complexes at various relative concentration of surfactant (below the CMC). Gelatin concentration was 0.5% (w/v) at 30 °C. The solid lines are best fit to the data. The binding curve of gelatin−surfactant complex in aqueous solution at 30 °C.

In order to understand the binding of surfactant to gelatin, one needs to look at the structure of gelatin critically. Macroscopically, gelatin is characterized as a random coil in dilute

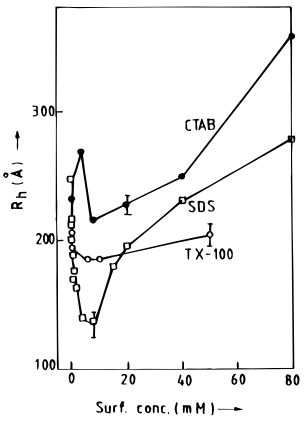

Figure 5. Hydrodynamic radius (R_h) of gelatin−surfactant complexes at various relative concentration of surfactant, for the entire range of concentrations. Gelatin concentration was 0.5% (w/v) at 30 °C. The solid lines are best fit to the data. The binding curve of gelatin−surfactant complex in aqueous solution at 30 °C.

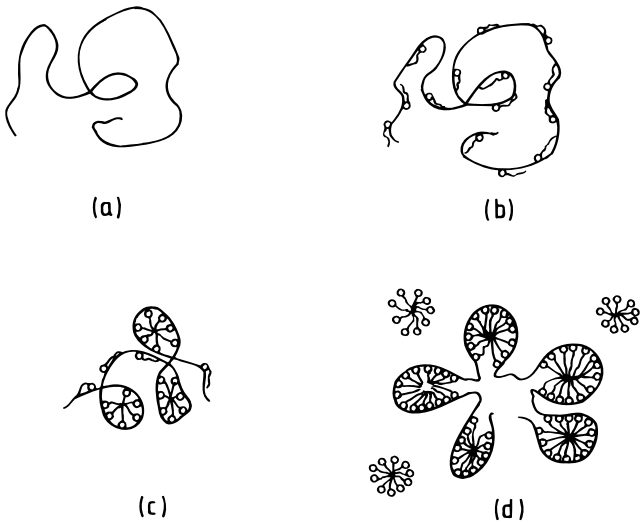

Figure 6. Model of gelatin−SDS/CTAB interactions at different surfactant concentrations. (a) Free gelatin chain, (b) specific binding of surfactant molecules to polar groups of gelatin chain, (c) induced micellization causing reduction (for SDS)/expansion (for CTAB) surfactant up to CAC, and (d) gelatin−surfactant complex coexisting with free micelles above CMC.

solutions with a persistence length[22,23] ∼ 20 Å, $R_g \approx 330$ Å, and $R_h \approx 220$ Å. This biopolymer is a polypeptide with the monomeric representation $-(\text{Gly}-\text{X}-\text{Pro})_n-$ where X represents the amino acid residues, mostly lysine and arganine ∼7.5%, glutamic acid and aspartic acid ∼12%, and leucine, iso-leucine, methionine, and valine ∼6%. One-third of the chain comprises of glycine ∼33% and another one-third is either proline or hydroxyproline ∼22%. The rest are other residues present in trace amounts. This implies that, at neutral pH, about 7.5% of the gelatin molecule is positively charged (lysine and arganine), 12% is negatively charged (glutamic and aspartic acid), and 6% of the chain is hydrophohic in nature (comprising leucine, isoleucine, methionine, and valine) leaving about 58% of the chain comprising glycine, proline, and hydroxyproline to be neutral.

(i) Gelatin−SDS Interactions. Results for the gelatin−SDS system show that there is a decrease in the hydrodynamic radius up to 8 mM conc (CMC of pure SDS), implying a contraction of the coil size leading to the formation of a more compact coil. The picture which can be conjectured is that initially monomers of SDS interact electrostatically with the oppositely charged sites of polymer chain. This reduces the electrostatic repulsion within the polymer molecule, and as a result, coiling of chain starts. Such coiling may bring the hydrophobic part of the surfactant closer together, resulting in aggregates of bound surfactant molecules (monomers). Thus a micelle-like structure is formed or there is induced micellization, further increasing the coiling and reducing the size. This phenomena is seen up to a surfactant concentration of 8 mM. Beyond this there was continuous increase in the radius of the gelatin−SDS complexes. Since micelles get formed for surfactant concentrations above CMC value, now the interaction is mostly between SDS micelles and gelatin chains resulting in an expansion of the chain stablized through necklace-bead model.[15] Now the polymer−SDS complex and SDS micelles coexist together. Radii of the micelles measured through the double exponential fitting, were found to be ≈12−30 Å. SDS is known to form much bigger micelles (these at ∼4 CMC are typically ∼20 Å) in aqueous environment,[25,26] but the presence of gelatin inhibited this process as per our studies.

Hence, our studies revealed that, up to 4 mM concentration of SDS, it was mostly specific binding of SDS polar head to high-energy positively charged sites of gelatin molecules, with the net effect leading to the shrinking of the gelatin chain by ∼30%. No free micelles could be detected here. Next, noncooperative binding prevailed up to 10 mM of surfactant concentration where the size change was marginal ≤10%. Beyond this concentration and up to 100 mM concentration of SDS, the chains expanded due to the formation of necklace-bead structures and this region of binding is often referred to as cooperative binding domain. Above 4 mM concentration of SDS, the surfactant micelles were found to coexist with the gelatin−SDS complexes in thermal equilibrium. Though these micelles did not grow beyond $R_h \simeq 30$ Å, the $g_1(\tau)$ function always exhibited a double-exponential behavior, implying the presence of these micelles at all SDS concentrations above 4 mM. We identify this as critical association concentration (CAC). The model described above is shown in Figure 6.

On the basis of purely geometrical considerations, one can deduce the saturation binding concentration of SDS to gelatin. The gelatin chain has a typical [22,23] $R_g \sim 350$ Å, cross-sectional radius $r = 3$ Å, hence the end-to-end length $R_e = \sqrt{6}R_g = 810$ Å. This gives the surface area of the chain as $2\pi r R_e \simeq 16200$ (Å)^2. As has already been discussed, only 7.5% of gelatin chain is positively charged giving the positively charged surface area to be ∼1215 (Å)^2. We used a gelatin concentration of 0.5% (w/v) where gelatin had a molecular weight $\sim 2 \times 10^5$ daltons. So, there were 15×10^{18} molecules of gelatin in the solution with total positively charged surface area $\sim 1.82 \times 10^{22}$ (Å)^2. One SDS molecule effectively covers[27,28] an area of 64 (Å)^2, thus $\sim 2.85 \times 10^{20}$ molecules or, equivalently, a concentration of 0.47 mM of SDS is needed to cover all the available positively charged surface area allowing close packing. Hence, the coulombic binding between polar heads of SDS and positively charged binding sites of gelatin molecule cannot possibly occur beyond this critical concentration. Our experimental result (CAC = 4 mM) is off from this over simplified picture by a factor of 10. The typical saturation binding ratio calculated from above is SDS:gelatin = 0.027g:1g. This is at best an indicative figure valid under close packing conditions. It has been established earlier that this ratio is 1.4 g:1 g for most of the SDS−protein complexes, and it extends to 2 g:1 g in the case of reduced proteins.[15] The observed low weight ratio necessitates further probing of this system.

(ii) Gelatin−CTAB Interactions. Variation of hydrodynamic radius (R_h) of gelatin−CTAB complexes with CTAB

concentration clearly indicates that there was marginal expansion of the chain ≤10% up to the surfactant concentration 4 mM; this was a behavior opposite to that of SDS. Assuming the nature of interaction to be same as in SDS (i.e., electrostatic and hydrophobic), the expansion could be due to electrostatic repulsion between the positive sites of chain and bulky cationic head groups as well as a longer chain associated with CTAB as compared to SDS molecule. Hydrophobic interaction may be operating between the hydrohobic part of CTAB and hydrophobic sites on the gelatin chain. Thus induced micellization was found to be absent in this case. Further increase in size was observed beyond 8 mM concentration of CTAB was due to the formation of polymer−micelle complex. Our results showed that the specific binding between CTAB and negatively charged binding sites of gelatin chain was rather marginal which produced a small (≤10%) increase in the size of the chain up to 2 mM concentration of CTAB. Beyond this concentration, the size of the gelatin−CTAB complex grew steadily, and at a concentration of 80 mM of CTAB the complex had a size of 360 Å. This happened mostly due to the formation of necklace-bead structures through cooperative binding. Here 2 mM appears to be the critical association concentration (CAC), and at all concentrations higher than this value, the presence of CTAB micelles were clearly observed from the behavior of $g_1(\tau)$ data. Though the CTAB concentration was raised from 0.4 to 80 mM (200 times), these micelles did not grow beyond $R_h \sim 40$ Å, thereby implying the inhibition effect of gelatin on CTAB micellar formation. The model described above is depicted in Figure 6.

Following the calculations presented for the case of SDS, one can deduce the saturation binding concentration of CTAB to gelatin. About 12% of the gelatin is composed of negatively charged binding sites. And like SDS, CTAB also covers an effective surface area of 64 $(Å)^2$ upon binding.[27,28] The total negatively charged surface area available on gelatin chains in a 0.5% (w/v) solution is, thus, $\sim 2.9 \times 10^{22}$ $(Å)^2$. Hence, a CTAB concentration ~0.76 mM is required to saturate all binding sites in close-packing arrangement. So, high-energy specific binding should occur below 0.76 mM concentration of CTAB according to this simplified picture. In our case this was observed up to a concentration ~0.2 mM. Hence, for this surfactant we observed the specific binding up to a concentration of 0.2 mM, and beyond this, cooperative binding to gelatin molecules dominated the interaction process. The noncooperative binding was either absent or could not be observed. The CTAB micelles had a typical hydrodynamic radius ~ 24 Å at 0.4 mM surfactant concentration which increased to ~40 Å at 80 mM concentration. The saturation binding ratio calculated from above is CTAB:gelatin = 0.055g:1g. This is again an indicative figure applicable under close-packing conditions.

(iii) Gelatin−TX-100 Interactions. Data of TX-100 (Table 3) shows that initially there was a slight increase in the radius of the gelatin-TX 100 complex up to 2 mM concentration of the surfactant after that these values remained almost constant at ≈220 Å approximately at a value equal to the size of free gelatin coil. The most likely explanation is that, since TX-100 has no charged head group, electrostatic interactions (attractive or repulsive or both) are not present. Hence, there was hydrophobic interaction only which led to slight increase in the size initially. The micelles of this surfactant formed in the gelatin solution had a typical size of ~14 Å at all concentrations studied. This implied that higher concentrations of this surfactant had absolutely no effect on the micellization phenomena. A conjecture based on our observations is shown in Figure 7.

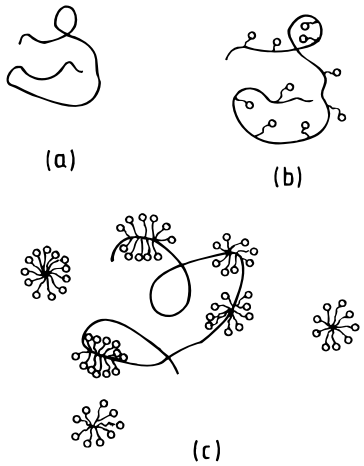

Figure 7. Model of gelatin−TX-100 interactions at different surfactant concentrations. (a) Free gelatin chain, (b) specific binding of surfactant molecules to hydrophobic groups of gelatin chain, and (c) gelatin−surfactant complex coexisting with free micelles above CMC.

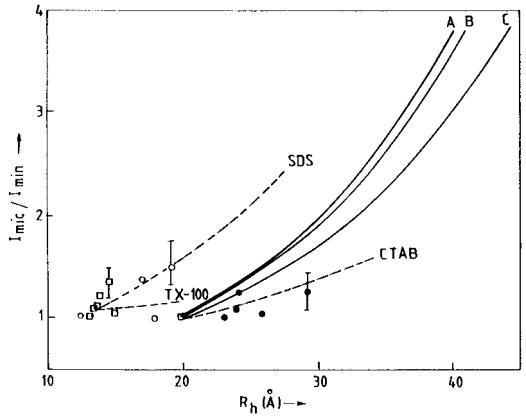

Figure 8. Variation of reduced scattered intensity I_{mic}/I_{min} with hydrodynamic radius R_h for surfactant micelles in gelatin−surfactant solutions at 30 °C. The solid lines are theoretical curves for spherical (A), oblate (B), and prolate (C) ellipsoid micelles. In curves B and C the values of the semiminor axes were fixed equal to 18 Å. Refer to ref 25 for details of these theoretical calculations.

(iv) Micellar Shapes. The intensity of light scattered from micelles can be written as[25−26]

$$I_{mic} \sim \frac{CMP(q)}{1 + 2A_2MC} + ... \qquad (7)$$

where $P(q)$ is the particle structure factor, M is micellar molecular weight, and A_2 is the second virial coefficient of excess chemical potential. If the smallest micelle (presumed to be a sphere), scatters an intensity I_{min}, one has

$$\frac{I_{mic}}{I_{min}} = \frac{M}{M_{min}P(q)} \qquad (8)$$

For a random coil the particle structure factor is given as $P(q) \simeq (1 - q^2R_g^2/3)$ for $qR_g \ll 1$. The theoretical curves can be computed for different micellar sizes (R_h-values) following the procedure of Mazer et. al.[25] for spherical and ellipsoidal micelles. These are shown in Figure 8. The values of I_{mic}/I_{min} are plotted against micellar size (R_h). The theoretical plots for spherical and ellipsoidal (oblate and prolate) micelles are shown to provide comparison to experimental data. For SDS samples, one finds the curve going almost parallel to that of the theoretically predicted curve for spherical micelles, thus implying the

possibilities of formation of sphere-like micelles in presence of gelatin. The micellar size grew from $R_h \simeq 12$ Å to 30 Å at the highest concentration of SDS studied (100 mM). At higher concentrations, SDS is known to form cylindrical micelles but the presence of gelatin apparantly did not facilitate the growth of these micelles beyond ~30 Å.

In the case of CTAB, the data is closer to the theoretical curve for a prolate ellipsoid over the concentration range studied in this experiment. The effective hydrodynamic radius almost doubles from ~23 Å at CMC to 40 Å at 100 mM concentration of CTAB, and the data shown in Figure 8 indicates that the CTAB micelles could be oblate ellipsoids in shape. Here, again the presence of a biopolymer (gelatin) has contributed to the process of nonformation of bigger micelles. For TX-100 samples, stable micelles were formed, typically with $R_h = 15$ Å, and these remained stable in size even when the concentration of TX-100 was raised to 50 mM.

IV. Conclusions

DLS studies revealed that both cationic and anionic surfactants bind specifically to appropriate polar groups of gelatin molecule altering the effective size of the biopolymer. SDS induced contraction of the chain up to the CAC (≈4 mM) by almost 30%, mostly following specific binding mechanism.[15] Beyond, CMC (≈8 mM), the cooperative binding prevailed leading to the formation of gelatin−SDS complexes that coexisted with free SDS micelles. In case of CTAB, the specific binding was found to be marginal which led to the expansion of the chain by ≤10% up to the CAC ≈ 0.2 mM. Beyond the CMC (≈0.4 mM), the cooperative binding prevailed and gelatin−CTAB complexes were found to be coexisting with free CTAB micelles. The hydrophobic binding dominating the gelatin and nonionic surfactant, TX-100 interactions did not affect the gelatin chain size significantly. On the basis of our results and the general formalism of polymer−surfactant interactions available in the literature,[15] we conclude that the necklace-bead model suits the geometrical description of gelatin−surfactant complexes. The significance of the low surfactant−protein binding ratio observed in these investigations calls for further probing of the kinetics of binding between gelatin and ionic surfactants.

Acknowledgment. This work was supported by grant from Department of Science and Technology, Government of India.

References and Notes

(1) Robb, I. D. In *Anionic Surfactants, Physical Chemistry of Surfactant Action*; Lucassen−Reyenders, E. H., Ed.; Surfactant Science Series, Vol.10; Marcel, Dekkar: New York, 1981; p 109.
(2) Goddard, E. D. *Colloids Surf.* **1986**, *19*, 1301.
(3) Hayakawa, K.; Kwak, J. C. T. In *Cationic Surfactants, Physical Chemistry*; Pulingh, D., Holland, P. M., Eds.; Dekker: New York, 1991.
(4) Nagarajan, R. *Colloids Surf.* **1985**, *13*, 1.
(5) Cabane, B. *J. Phys. Chem.* **1977**, *81*, 1639.
(6) Guo, X. H.; Zhao, N. M.; Chen, S. H.; Teixeira, J., *Biopolymers* **1990**, *29*, 335.
(7) Turro, N. J.; Lei, X.; Ananthapadmanabhan, K. P.; Aronson, M. *Langmuir* **1995**, *11*, 2525.
(8) Meewes, M.; Ricka, J.; de Silva, M.; Nyffenegger, R.; Binkert, Th. *Macromolecules* **1991**, *24*, 5811.
(9) Cabane, B.; Duplesseix, R. *J. Phys*. **1987**, *48*, 651.
(10) Walter, R.; Ricka, J.; Quellet, Ch.; Nyffenegger, R.; Binkert, Th. *Macromolecules* **1996**, *29*, 4019.
(11) Cosgrove, T.; White, S. J.; Zarbakhsh, A.; Heenan, R. K.; Howe, A. M. *Langmuir* **1995**, *11*, 744.
(12) Feitosa, E.; Brown, W.; Hansson, P. *Macromolecules* **1996**, *29*, 2169.
(13) Steinhardt, J.; Reynolds, J. A. *Multiple Equilibra in Proteins*; Academic Press: New York, 1969.
(14) Jones, M. N. *Chem. Soc. Rev*. **1992**, *21*, 127.
(15) Ananthapadmanabhan, K. P. In *Interactions of Surfactants with Polymers and Proteins*; Goddard, E. D., Ananthapadmanabhan, K. P., Eds.; CRC Press: Boca Raton, 1993; p 319.
(16) Pankhurst, K. G. *Surf. Chem. Res. Suppl.* (London) **1949**, *109*.
(17) Knox, W. J., Jr.; Wright, J. F. *J. Colloid Sci*. **1965**, *20*, 177.
(18) Kragh, A. M. *Trans. Faraday Soc*. **1964**, *60*, 22.
(19) Shone, M. T. *Nature* **1962**, *194*, 1235.
(20) Greener, J.; Contestable, B. A.; Bale, M. D. *Macromolecules* **1972**, *20*, 2490.
(21) Bohidar, H. B.; Berland, T.; Jossang, T.; Feder, J. *Rev. Sci. Instrum*. **1987**, *58*, 1422.
(22) Bohidar, H. B.; Jena, S. S. *J. Chem. Phys*. **1994**, *100*, 6888.
(23) Pezron, I.; Djabourov, M.; Leblond, J. *Polymer* **1991**, *32*, 3201.
(24) Pecora, R. *Dynamic Light Scattering*; Plenum: New York, 1985. Berne, B. J.; Pecora, R. *Dynamic Light Scattering*; Wiley-Interscience: New York, 1976.
(25) Mazer, N. A.; Benedek, G. B.; Carey, M. C. *J. Phys. Chem*. **1976**, *80*, 1075.
(26) Young, C. Y.; Missel, P. J.; Mazer, N. A.; Benedek, G. B.; Carey, M. C. *J. Phys. Chem*. **1978**, *82*, 1375.
(27) Israelachvili, J. N. In *Physics of Amphiphiles: Micelles, Vesicles and Microemulsions* Degiorgio, V., Corti, M., Eds.; North-Holland; Amsterdam 1985; p 24.
(28) Tanford, C. *The Hydrophobic Effect: Formation of Micelles and Biological Membranes*; Wiley-Interscience: New York, 1973.